Numerical Simulation and Design of COVID-19 Disease Detection System Based on Improved Computing Techniques

[1]Prince Choudhary, [2]Abhigya Saxena
[1]M. Tech Scholar, Department of Computer Science, YIT, Jaipur
[2]Assistant Professor, Department of Computer Science, YIT, Jaipur

Abstract

The high demand for testing the sickness has led to a lack of resources at emergency clinics as the coronavirus epidemic continues. PC vision-based frameworks can be used to increase the productivity of Coronavirus localization. However, a significant amount of information preparation is needed to create an accurate and reliable model, which is currently impractical given the peculiar nature of the illness. One such model is for differentiating pneumonia cases by using radiographs, and it has achieved sufficiently high exactness to be used on patients. Various models are currently being used inside the medical services sector to order different illnesses. This proposal evaluates the benefit of using motion learning to broaden the presentation of the Coronavirus location model, starting from the premise that there is limited information available for Coronavirus ID. Infections that affect the human lungs include viral pneumonia caused by the coronavirus and other viruses. The World Health Organization (W.H.O.) proclaimed Covid a pandemic in 2020; the sickness originated in China and quickly spread to other countries. Early diagnosis of infected patients aids in saving the patient's life and prevents the infection's further spread. As one of the quickest and least expensive methods for diagnosing the condition, the convolutional neural organization (CNN) model is suggested in this research study to assist in the early detection of the infection using chest X-Beam images. Two convolutional brain organizations (CNN) models were created using two different datasets. The primary model was created for double characterization using one of the datasets that only included pneumonia cases and common chest X-Beam images. The second model made use of the information advanced by the primary model using move learning and was created for three class divisions on chest X-Beam images of cases with the coronavirus, pneumonia, and regular cases.

Keywords – Image Processing, Covid-19, Deep Learning, CNN, ANN.

I. INTRODUCTION

The coronavirus, a respiratory condition that affects the human lungs, is currently declared a pandemic that is affecting the entire world. According to the World Health Organization, as of today, October 2, 2020, there have been more than 34 million actual cases, 23.9 million recoveries, and 1.02 million fatalities ("WHO Covid Infection (Coronavirus) Dashboard | WHO Covid Illness (Coronavirus) Dashboard," n.d.). Coronavirus first appeared in December 2019 in Wuhan, Hubei Province, China (Q. Li et al., 2020), from which it quickly spread to other countries. Early diagnosis is essential for both patients and the populations around them because the coronavirus infection is contagious; this way, the patient will receive proper care, and people will be protected. The best strategy for combating the coronavirus pandemic is to treat patients with the highest level of care and medicine as soon as they are diagnosed with the infection. Switch record polymerase chain response (RT-PCR) is typically used in the diagnosis of coronavirus; however,

because this method has low awareness in the early stages of illness, it could lead to more transmissions (L. Li et al., 2020). This test device is pricey and alerts, so for early detection chest X-rays and computer tomography (CT) tests are the best option to use in identifying any persistent that exhibits pneumonia side effects.

Both the master radiologist and those who are not radiologists need to complete this study. The framework is designed to help radiologists diagnose pneumonia and the coronavirus more accurately and quickly, hence it is crucial that they are proficient radiologists. Additionally, it helps persons without access to a radiologist to be evaluated early so that proper action can be taken before the contamination persists. This study advances the area of medicine by helping doctors diagnose the presence of the coronavirus and pneumonia quickly, as opposed to the traditional method, which involves a number of assessment procedures before cases are confirmed. This study also advances the field of artificial

intelligence by demonstrating the suitability of the deep learning model for the analysis of human illnesses.

The SARS-COV2 (Coronavirus) outbreak started in Wuhan City, China, in late 2019 and spread to other parts of the world. More than 220 countries and areas around the world are affected by the global coronavirus pandemic, which has profound effects on every aspect of our daily lives. As of January 22, 2022, there were a total of 34,64,64,304 (55, 85,224) contaminated (expired) Coronavirus cases reported worldwide [1]. The numbers of tainted cases increasing despite everything are generally increasing and don't show a particularly controlled condition. This disease has been classified as a widespread scourge by WHO, along with several controls used to increase the severity of this pandemic.

While the highly pathogenic illness typically affects patients by respiratory declines, it is disseminated through biological contact [5, 6]. Different investigations [7, 8] revealed that the SARS-CoV-2 spread by the oral-waste route, unlike other respiratory illnesses. A thorough analysis of stool samples from 71 persons who had the coronavirus and 39 people who tested positive for waste coronavirus RNA was completed in reference [9], supporting the idea that waste oral defilement might be another factor in the severity of the illness. Most commonly, coronavirus symptoms include weakness, fever, and hack [10–12].

Different gastrointestinal symptoms, such as loose stools, queasy feelings, and lack of appetite, might be seen in those who have been defiled [13, 14]. It's important to remember that disease transmission can happen without any symptoms, and that asymptomatic people might act as a source of contamination. Therefore, it is anticipated that strict adherence to the environment, hand hygiene, and contact isolation will assure viral control.

Coronavirus infections as well as other diseases that cause severe respiratory conditions [15]. It performs a real service in the management of heart physiology as well as the regulation of digestive disturbances. Nevertheless, it has been asserted that ACE2 is a viral RNA segment-interacting cell-surface receptor for contamination that functions in the lungs [16, 17].

RT-PCR is frequently used to confirm the presence of coronavirus. RNA rather than DNA is used as the underlying step in this biological reaction [18]. In order to make a comparing single abandoned DNA in the opposite record measure, the opposing transcriptase compound uses the RNA. The newly required single DNA is then converted into double-stranded DNA since it will be utilized to organize a PCR response [19, 20]. Despite numerous initiatives aimed at

increasing the number of PCR tests performed each day, this approach has a few cutoff thresholds. The startling rapidity of false negatives detected in individuals identifying the Coronavirus, the closed nature of PCR reagent units, and the generally lengthy time connection of this method [21].

II. OBJECTIVES

"To establish a completely programmed structure to differentiate and detect severity degrees of Coronavirus using radiographic photos and assess its exhibition" is the stated objective of the examination effort.

- To detect the presence of the coronavirus using artificial intelligence and the picture cushioning technique in chest X-ray images.
- To examine the details in X-ray sweep images and chest radiographs for the presence of the coronavirus.
- To describe the illness sharpness of the Coronavirus tests' CT filter images using the picture division process.

III. LITERATURE REVIEW

Koppen, J., A. Bhandari, and M. Agzarian (2020) The introduction of quantitative picture analysis has given rise to disciplines like radiomics, which have been used to predict clinical repercussions. A growing topic of interest for research is glioblastoma multiforme, a type of brain cancer (GBM). In the investigation of this disease, cancer division is an important step that is ready to go. Manual division is frequently ambiguous since it varies between observers. To combat this problem, robotized division has been proposed. The writer has shown interest in systems such as convolutional brain organizations (CNNs), which are AI pipelines displayed on the natural course of neurons (called hubs) and neurotransmitters (called associations). We investigate CNNs in order to better understand their role in the division of brain tumors, and we then do a writing search to determine a good pipeline for division. Then, by looking into a novel field called radiomics, we examine the potential uses of CNNs. In order to predict clinical outcomes, such as resistance and response to treatment, this study examines quantitative features of cerebral tumors, such as form, surface, and sign power [1].

McCann MT, Froustey E, Unser M, and Jin KH (2017) In this study, we suggest a novel, deep convolutional brain organization (CNN)-based calculation for handling poorly presented converse situations. In the past few years, regularized iterative calculations have become the de facto method for handling badly presented reversal problems.

These methods yield excellent results, but they can be difficult to implement in the long run because to factors including the difficulty in determining the hyperparameters and the high computing cost of the forward and adjacent administrators. The premise of this study is that unrolled iterative approaches, which involve sifting and pointwise nonlinearity, have the characteristics of a CNN, yet the typical administrator of a forward model is a convolution (H*H, where H* is the adjoint of H, the forward imaging administrator). We suggest using direct reversal followed by a CNN to address common convolutional backwards difficulties in light of this perspective. The instantaneous reversal embodies the true model of the framework, but when the issue is poorly represented, it causes artifacts. The CNN combines multiresolution decay and persistent learning to figure out how to get rid of these artifacts while preserving picture structure. In both genuine trial sinograms and fabricated apparitions, we demonstrate the suggested network's display in sparse view replication (down to 50 perspectives) on an equal bar X-beam processed tomography. For the more rational ghosts, the suggested network outperforms complete variety regularized iterative reproduction and takes less than one second to duplicate a 512 512 image on the GPU [2].

Nishio M, Yamashita R, Do RKG, and Togashi K (2018) Convolutional brain organization (CBO), a subclass of fictitious neural networks that has gained popularity in numerous PC vision projects, is generating attention in a variety of fields, including radiology. CNN uses a variety of structural building blocks, such as convolution layers, pooling layers, and totally associated layers, to organically and adaptively learn the spatial ordering of components through backpropagation. This survey article provides a viewpoint on CNN's core concepts and how they are applied to various radiological tasks. It also looks at CNN's challenges and potential directions in the field of radiology. This post will also discuss two techniques for using CNN to do radiological tasks: minimal dataset and overfitting, as well as ways to prevent them. Knowing the concepts, advantages, and limitations of CNN is essential for influencing its potential in symptomatic radiology, with the entire purpose to broaden radiologists' presentations and advance patient consideration [3].

Lakshmi Priya and Angulakshmi (2017) The process of separating abnormal tissues from common tissues, including as white matter (WM), black matter (GM), and cerebrospinal fluid, is known as "programmed division of cerebrum cancer" (CSF). Due to the heterogeneity of shape, region, and size of the cancer division, the course of division is still challenging. Positron discharge tomography (PET) images, PC Tomography (CT) images, and Attractive Reverberation Images are used to acquire the metabolic cycle, mental interaction, and itemized data of the images (X-ray). For exact cerebrum cancer division, multimodal imaging techniques (such PET/CT and PET/X-ray) that combine the data from numerous imaging processes give another option. This article provides a thorough overview of late programmed cerebrum growth division techniques using X-ray, PET, CT, and multimodal imaging techniques. This article [4] examines the strategy, methods, functional standards, advantages, obstacles, and future difficulties.

Nguyen HS, Doan NB, Best B, and others (2019) An unfavorable visualization is predicted by glioblastoma (GB) and its variants. The primary cause of death (COD) is related to the progression of the disease, but a significant portion is related to other factors. Because GB is a fundamental ailment that necessitates fundamental treatment, center with respect to all COD provides a thorough description of the condition. For individuals with cranial GB and its variations, The Diviner 18 was questioned. Age, orientation, race, marital status, characteristics of the malignancy, details of the therapy, and follow-up data were gathered. The patients were divided into two groups: group A (whose death was attributed to this malignant growth discovery) and group B. (passing ascribed to causes other than this disease determination). Between 1973 and 2013, lot A consisted of 36,632 deaths (94%) and bunch B of 2,324 deaths (5.9%). The final alternative mostly showed lower extents older than 60, Caucasians, married status, parts of the front facing/cerebrum stem/ventricle malignancy, and radiation exposure. Age >60, male orientation, race, not married, growth area, and no radiation were crucial free indicators for bunch B during a strategic relapse. Heart disease, respiratory disorders including the flu and pneumonia, cerebrovascular diseases, accidents and negative effects, and diseases are the most often realized CODs in group B [5].

IV. METHODOLOGY

The goal of this work is to produce a calculation that can analyze instances of pneumonia and the coronavirus from chest X-ray images. The Tensor handling unit (TPU), which serves as the equipment that processes the calculation, is used in the execution of the profound learning calculation explicitly. To cut down on overfitting, improve computation accuracy, and reduce actual preparation time, move learning is used for highlight extraction. The model execution process consists of the following four basic phases:
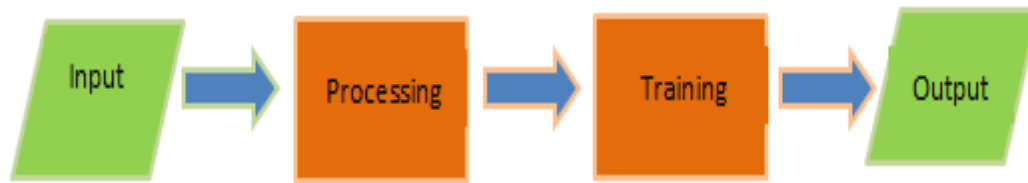
Figure 4.1 Block Diagram of the Design Stages

Stage of input: The model's contribution consists of RGB chest X-beam images with a PNG design. The main portion of the calculation is at this point. The model will start the subsequent stage, known as the pre-handling stage, after the X-beam images have been fed to it. Pre-handling stage: This is the second step of the calculation, where the information chest X-beam images are checked to see if they are in RGB structure or not. If not, they are completely converted to RGB structure, the X-beam images are then resized to 180 by 180, and finally, they are standardized by dividing each information image pixel by 255, making the pixels go from 0 to 1, instead of 0 to 225 which is the first range of pi. The preprocessing stage helps the computation quickly learn and concentrate on the most important picture highlights. The third stage of the model is the training stage. The pre-processed chest X-beam images are fed into the information layer of the convolutional brain organization (CNN) at this point, where highlights are learned and eliminated, before the output of the final secret layer passes the image on to the result layer. Stage of output: This is the final and final step in the model. By giving three different result classes—coronavirus, pneumonia, and typical—the organization's yield layer makes a final decision on the model. The convolutional brain network's final layer, which has a likelihood structure, is where this decision was made. When a class of coronaviruses has a higher likely esteem, that class is chosen for the computation. Alternatively, in the event that a class of pneumoniae has a higher likelihood esteem, that class is also chosen for the calculation.

System Architecture
Fig. 4.2's summary of the system architecture covers the processes listed below.

- The base model for the examination model engineering using move learning techniques was a pre-prepared model (base model) that was created

with a dataset of only pneumonia and common X-Beam images.

- The exploration dataset, which includes X-Beam images of everyday life and images of pneumonia and coronavirus, has been preprocessed and is now ready for the preparation step.
- The preprocessed chest X-beam images of cases with the coronavirus, pneumonia, and regular cases were used to create the proposed model design.
- The model output is a dynamic component of the model design that might be either the X-Beam image of pneumonia, coronavirus, or typical cases.

Dataset
All of the datasets used in this investigation study were obtained (downloaded) from the Kaggle dataset library thanks to Google's recent launch of 25 million free datasets at the beginning of this year. 2018 (Kermany et al.) is First, back chest X-beam images of pediatric patients old enough to range from one to five years of age were selected from Guangzhou women and children's clinical center. The chest X-beam images were screened to remove any X-Beam images that were jumbled or had poor quality outputs. Two expert radiologists examine and evaluate the discovery (Mark). To avoid errors, the third expert radiologist also checks the validity of the judgment. The dataset is divided into three parts: preparation, approval, and testing. Each of these parts is further sub-divided by two classes: typical and pneumonia. The dataset includes cases of viral and bacterial pneumonia, which are collectively referred to as the pneumonia class. 4,185 chest X-beam images were used to prepare the information, 1,047 images were used for approval, and 624 images were used for testing, of which 390 were cases of pneumonia and 234 were ordinary cases.
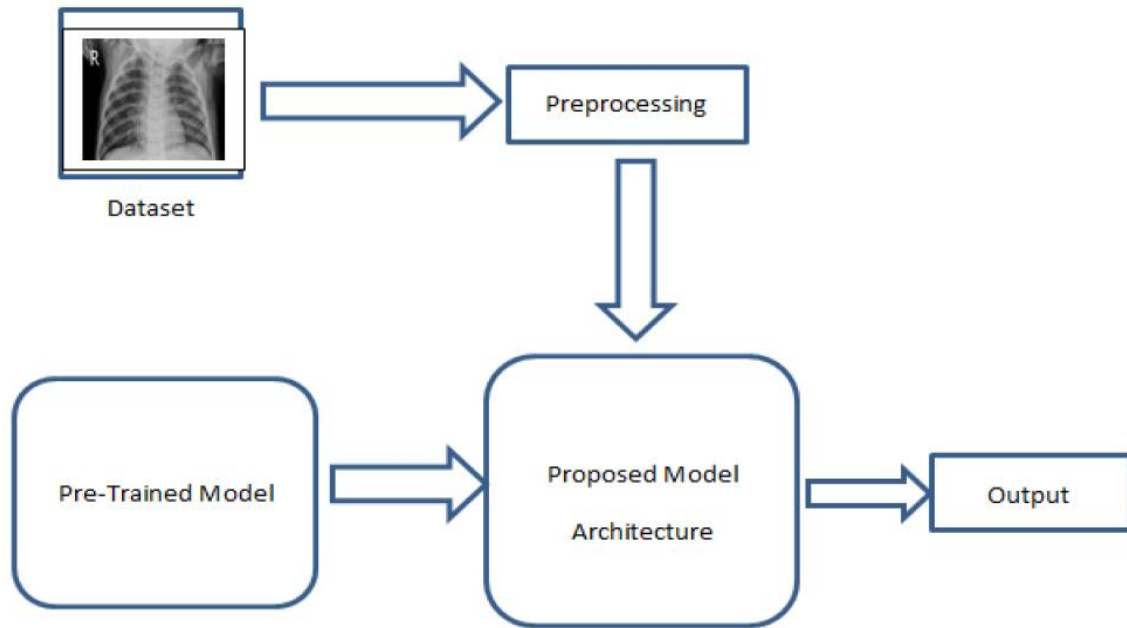
_____

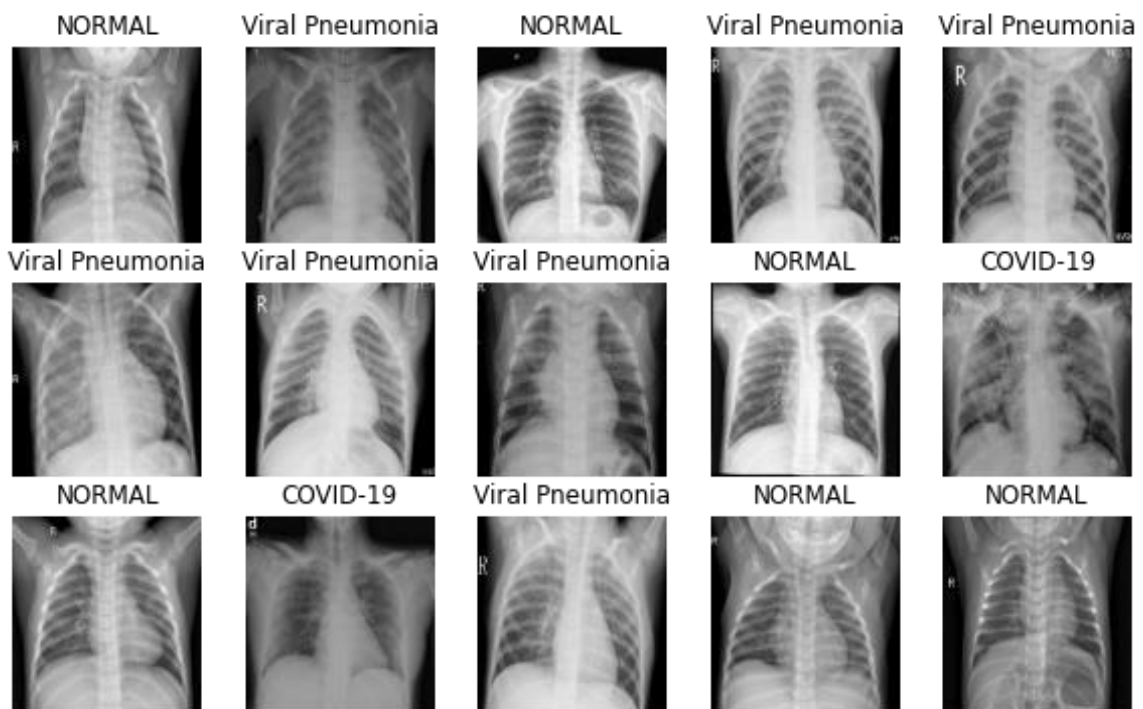**Figure 4.2 System Architecture**

Figure 4.3 COVID-19/Pneumonia/Normal Chest Images

The figure below shows COVID-19/Pneumonia/Normal class distribution in the training, validation, and testing part of the dataset in form of a bar chart.
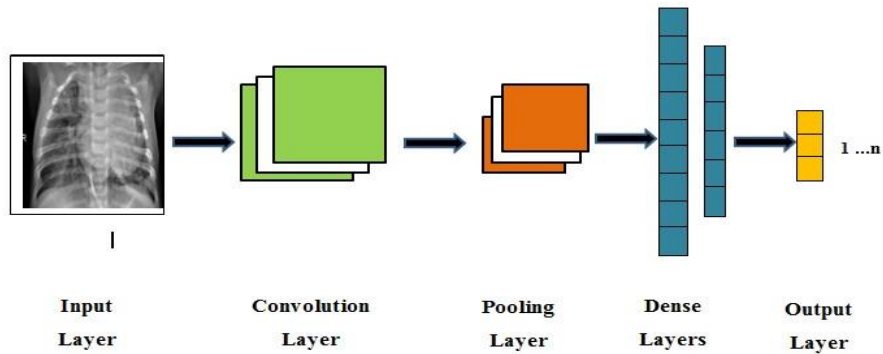
_____

Figure 4.4 Convolutional Neural Network Architecture

Activation Functions

A brain network layer's enactment capability determines whether or not a result will be passed to the next layer. Each layer of the brain organization is completed with the addition of the initiation capacity (NN). To determine the outcome of each brain network layer, direct and nonlinear initiation capabilities are used. The abilities that are mostly used in brain organizations and in-depth learning computations are nonlinear enactment abilities. The five most often used enactment capabilities will be highlighted in this investigation. Those are: function of sigmoid activation The activation function of the hyperbolic tangent (tanh)

Activation of Rectified Linear Units (ReLu) Activation of Softmax, and Function for activating the exponential linear unit (Elu)

Transfer learning

In tasks involving computer vision, the transfer learning method is typically and most frequently utilized. The following are some benefits of transfer learning: It cut down on a model's training period. The cost of computation was decreased. It avoids or lessens the over-fitting of models. With only a modest amount of data, it enables the training of huge CNNs. Additionally, it improves or degrades a mo
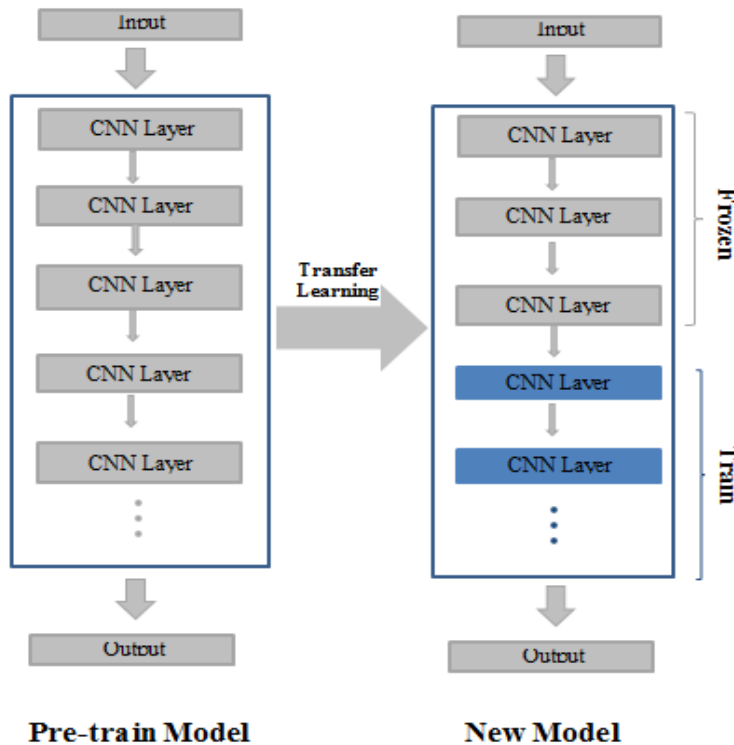

Figure 4.5 Transfer Learning Structure

Networks called assessment grids are used to quantify how well AI or deep learning models are presented. There are numerous types of evaluation grids that can be used to evaluate models. To evaluate the presentation of various models in relation to the most urgent issue, various assessment networks are used. While some assessment grids are appropriate for characterization models, others are best for assessing the presentation of relapse models. There are many different types of evaluation lattices, and this proposal research will highlight the ones that are most frequently used in the current study field. These are as follows: Complexity matrix Accuracy Recall Precision F1 ranking, and region beneath the rock curve (AUC).

V. RESULT ANALYSIS

The chest X-ray data was obtained from various Kaggle sources. The dataset includes various X-ray types as well as a fake metadata file that contains information on the name, age, sex, diagnosis, and other specifics of the patients. It consists of chest MRI scans that show no contamination or pneumonia. Downloading and transferring these two datasets into MATLAB.

The data is filtered for the dataset to only include the samples that have been tested positively for the coronavirus and have a pont front (dad) view. There are 206 total chest x-beam images of the coronavirus. The dataset is further divided into a train and approval group with an 80:20 ratio.

Table 5.1
Analysis of Dataset

Images	COVID-19	Normal	Total
Train	165	165	330
Validation	41	41	82
Total	206	206	412

Pictures of the Coronavirus and Common Chest X-ray can be found in the dataset. In order to distinguish between typical chest X-rays and individuals with coronavirus contamination, a CNN model with two classes needs to be created. Here are separate test chest images for patients with Coronavirus and Regular people.

Matlab programs can be written and run on the program to create the CNN model. The dataset is converted into a compressed record to save space before being sent to Dropbex. Google Colab shares the Dropbox interface, which downloads the compressed document quickly.

Convolutional layers and Completely Associated Layers are the two different types of layers used in the CNN model. A multi-layered GNN model is created, consisting of two fully related layers for arranging Coronavirus and standard x-beam images, followed by three configurations of stacked convolutional and pooling layers. There are four convolutional layers with channel sizes of 3x3, although the channel counts increase over the layers to 32, 64, 64, and 128.
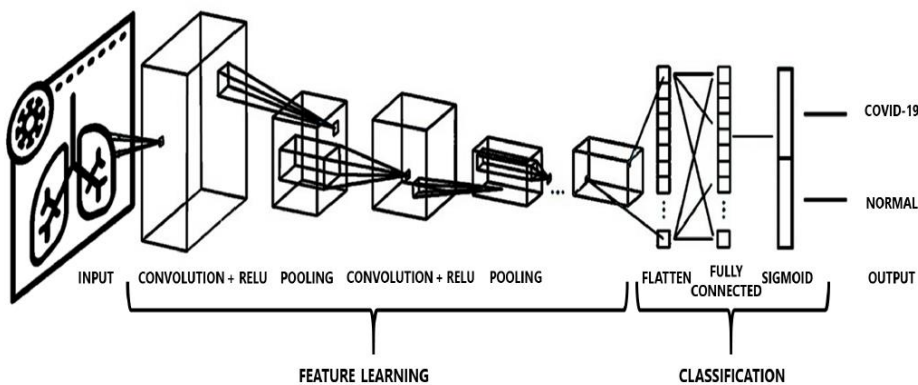

Figure 5.1 Architecture of Proposed Model

This model is built without any preparation and uses 56 lakh boundaries in total. The initial information shape is 224 x 224, however after the first convolutional layer, it transforms into 222 x 222. Prior to the smoothing layer, the form is altered to 26 x 26 or 26 x 128. The dataset is prepared using the built-in Keras Picture Generator package. The dataset is rescaled for standardization of RGB images by 1/255 to aid in information combining. Different models demand a minimum of 3000 images for preparation in order to provide a respectable exactness score.
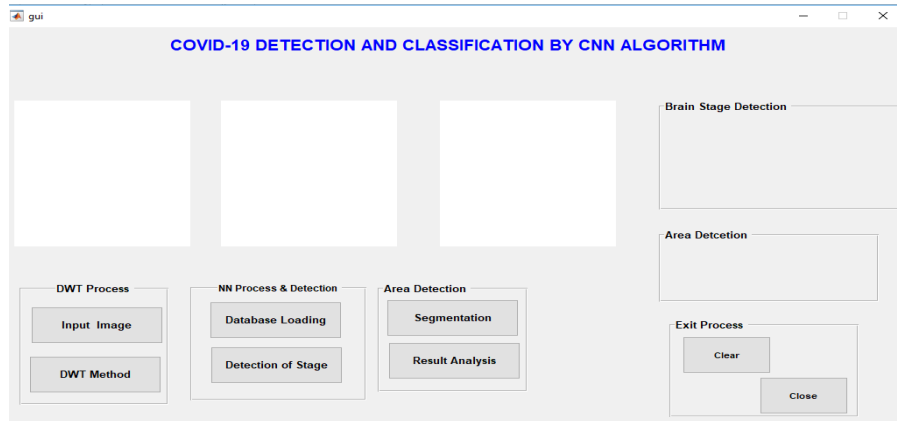
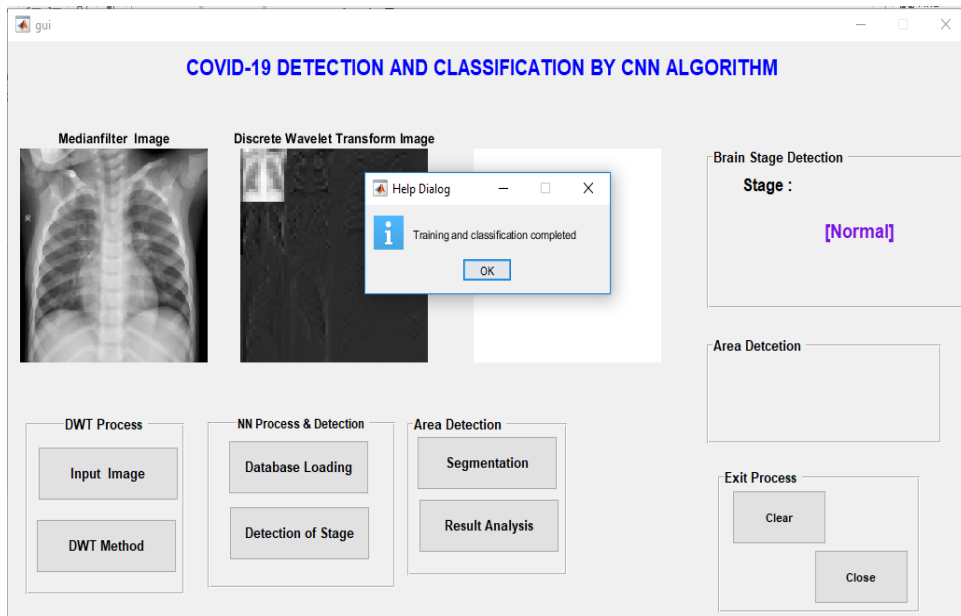**Figure 5.2 Architecture of GUI for Proposed Model**

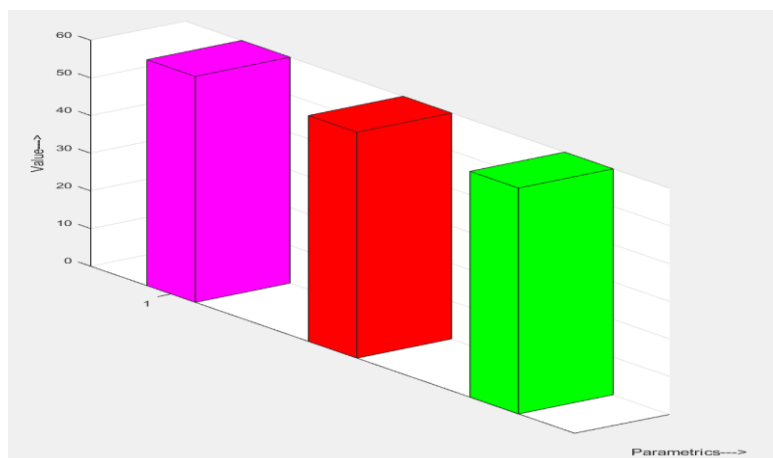**Figure 5.3 Process of Proposed Methodology**

Figure 5.4 Specificity, Accuracy and Sensitivity Analysis of Segmentation

Analysis of Accuracy

A confusion matrix is produced to provide a summary of the findings on a classification problem and to provide a visual representation of the model's findings. It summarizes the forecasts, split down by class, that were right and wrong. It demonstrates how the classification model becomes perplexed when it makes predictions and provides information on both the size and the nature of the errors that are created..

Table 5.2
Confusion Matrix Overview

	COVID-19	NORMAL
COVID-19	True Positive	False Negative
NORMAL	False Positive	Irue Negative

The Accuracy, Misclassification Erroc, Sensitivity Specificity and Precision of the model are evahuated from the Confusion Matrix to get a deeper understanding about model fitting [D].

Accuracy: Accuracy is used to measure the magritude of the correctly predicted classes. It calculates how many COVID-19 and Normal patients have been correctly classified respectively. The formula is given as:

$$\text{Precision} = \frac{TP + TN}{n}$$

The confusion matrix has been performed on the Validation dataset. The results of the confusion matrix are as follow:
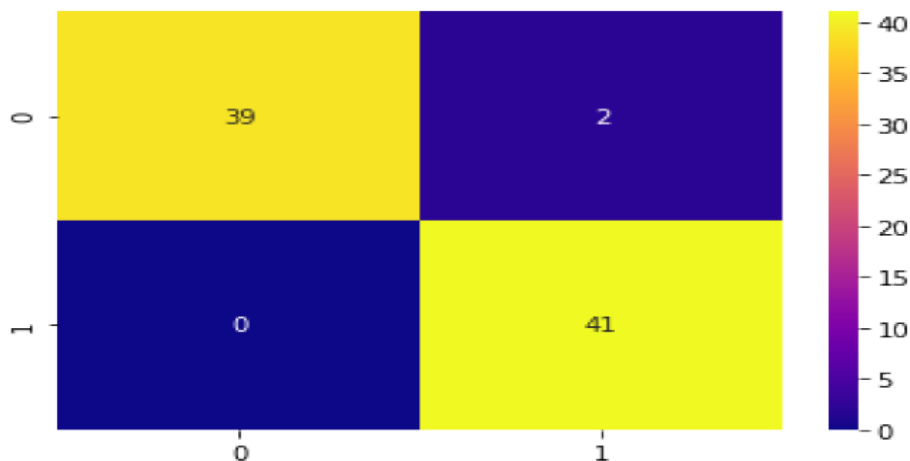

Figure 5.5 Confusion Matrix

On decoding the Confusion matrix, it is observed that out of 41 COVD-19 affected patients, there are two patients wrongly classified and, out of 41 Normal patients, 0 patients have been wrongly classified. In our model, 2 of the patients have been wrongly classified in total.

Table 5.3
Analysis of Results

Accur acy	Misclassific ation Error	Sensiti vity	Specifi city	Precis ion
0.912	0.0143	0.922	1.000	1.000

A model uses more than one age when using profound learning because the model's accuracy and misfortune may alter over time. Figure 5.4 illustrates the model's accuracy and demonstrates that it cannot cluster important forecasts first.

Given that the preparation and approval precision deteriorates over time and is rarely enlarged at specific ages, it fits the dataset perfectly after a few years. The approval precision initially increased in a straight line, but with time it started to become consistent as the gap between the preparation and approval precision shrank. This implies that the model has very little evidence of over-fitting and has produced excellent accuracy results over time.

VI.   CONCLUSION & FUTURE SCOPE

To sum up, the research was focused on developing a framework that can aid radiologists in accurately diagnosing cases of pneumonia and the Coronavirus during this challenging pandemic season. In order to identify these infections as quickly as possible, CNN computations were used as shown in the system area. We have demonstrated how the exchange learning approach was used to get over these

---

problems despite the lack of Coronavirus information. The core model was created for paired characterisation (pneumonia/ordinary) on the first dataset, which contains only pneumonia patients and typical CXR images. As it makes sense, two CNN calculations were prepared with two special datasets. The main model serves as the base model for the second model, which was created using the exchange learning technique, and was based on the second dataset, which includes images of the common cases for the three classes (coronavirus, pneumonia, and so on) (Coronavirus, pneumonia, and typical). One of the biggest disruptions to many people's lives over the past two years has been the coronavirus. One way we can help in the diagnosis of the Coronavirus and other illnesses is via chest X-rays. Many complex neural networks have been created to try to accomplish that. The CNN suggested in this study manages to achieve a 91.38 percent exactness with an AUC of 93.46 percent; great effort has been taken to demonstrate those successful examples. Future research may get us closer to the goal of having a model that can be used therapeutically for determination purposes, even though it is not one yet. This investigation has a lot of potential future extensions. Executing additional structures is the primary advancement. In order to prepare more complex designs, I might want to look into options for model preparation that provide a larger GPU memory limit. This would enable the use of origin modules despite several deep layers. The distribution of various infections is the next potential research topic. This would enable an inquiry into the hypothesis that different models are best for different diseases. If so, more research could be able to explain why there are differences in how different illnesses perform. Different information-partitioning techniques, including k-overlap information splitting, could also be used. This would further validate the results and provide insight into the effects of information predilection on effectively developing a model.

REFERENCES

[1.] World Health Organization. https : / / ww , who . int/ emergencies/diseasas/ novel coranav irus-2019/question- and-answors-hub/q-a-dotail/q-a-coronavirusaes.

[2.] A Trief History of Coronaviruses. httpa: // thaconversation - con / coronavirusas - a briaf-hiatory-135506.

[3.] Shuai Wang et al. A deep learning algorithm using CTr images to screen for Corona Virus Disease (CONID-19). In: MedRxio (2020).

[4.] Ali Narin, Ceren Kaya, and Ziynet Pamuk Automatic detection of coronaviras disease (covid-19) using x-ray imsges and deep cotvolutional reural networks. In: ω Xivo preprint wXic 2003.10849 (2020). 51235105

[5.] Nuno Femandes. Economic effects of coronavirus outbreak (COVID-19) on the world economy. Irr Avilable at SSRN 3557504 (2020).

[6.] What a Coronavirus daes to the Bady. https: / / wru. natianalgaographic. con/ acionce/ 2020/02/here-is-what-coranav irus-does-to-tha-body/-

[7.] Tests may miss more than 1 in 5 Covid-19 Cases. httpa: // ww . modicalnowstoday . con/ articloag/ tasts-may-misa-more-than-1-in-5-covid-19- casen.

[8.] Pepsi M, B. B. ., V. . S, and A. . A. "Tree Based Boosting Algorithm to Tackle the Overfitting in Healthcare Data". International Journal on Recent and Innovation Trends in Computing and Communication, vol. 10, no. 5, May 2022, pp. 41-47, doi:10.17762/ijritcc.v10i5.5552.

[9.] Zi Yoe Zun et al. Coronavirus disease 2019 (COVID-19) a perspective from Chira. In: Rantiology (2020), P. 200490.

[10.] Hayit Greenspar, Bram Van Ginneken, and Ronald M Summers. Guest editorial deep lesrruing in medical imaging: Overview and future promise of an exciting new techrique. Irc IEEE Transactions on Medion IMaxing 35.5 (2016). PP. 1153-1159.

[11.] Halgurd S Maghidid et al. Diagnosing CONID-19 pre umonia from X-ray and CI' images using deep learming and transfer learning algorithms. In: arXiv preprint a Xiv:2004.00038 (202D).

[12.] Ioannis D Apostolopoulos and Trani A Mpesiana. Covid-19: automatic detection from x-ray imapes utilizing transfer karrung with convolutional neural networks. Ire Physionl and Engineering Scionces in Meaicine (2020), p. 1.

[13.] Asmaa Abbas, Mohammed M Abdelsames, and Mohamed Medhat Gaber. Classification of COVID-19 in chent X-ray images using DelfraC deep convolutional reural network In: arXio preprint a Xiv:200313815 (2020).

[14.] Sanhita Bosu and Sushamita Mitra. Deep Learning for Screening COVID-19 using Chest X-Ray lmages, Irr arXio preprint ɷJXiz 2004.10507 (2020).

[15.] Fei Shan et al. Lang infection quantification of covid-19 in ct images with deep learning. Irc ar Xio prequint arXim:200304655 (2020).

[16.] Xiaowei Xu et al. A Deep Learning System to Sereen Novel Coronavirus Disease 2019 Preumonia. Irr Engineding (2020).

[17.] An intuatioe Explanation of Condodutional Newrat Netionks. httpa: // ujjulkarn. ma/ 2016/ og/11/intuitive-axplanation-convnata/.

[18.] Demystifying the Mathonatics Eatuind Conoductionat Neard Networks (CNNs). //www.analyticavidhya.con/blog/2020/02/matherica-behind-canvolutional-neuralnotwork/?utm_aource-

_____

blogkutn_sourco-1earn-inaga-clasaification-con-convolutiona noural-networks-5-datanates.

[19.] GNN Fram Sortch - Mathonatics. httpa :// couraas - analyticavidhya - can/coureas/ convolutional -naural-natworks - conn-from-Bcratch?utn__ourca-blogkutm_nodiumnathanatica-behind-convolutional-naural-notwork.

[20.] Muhammad Imran Raxzak, Soeeda Naz, and Ahmsd Zaib. Deep learning for medical image processing: Overview, challenges and the future. In: Qassfiontion in BiaApps. Springer, 2018, pp. $323 - 350$

[21.] GNN Architedifure Forging Prehmays for the Future https ://miasinglink - ai / guidas/ convolutional - noural - netwarks/ convolutional - naural - network - architecturaforging-pathays-futura/-

[22.] Math of CNN. https:// qiita . con/ Horring0914/ itens / a815ca24427974030526#2activation-1ayar.

[23.] GNN Math Model. httpa://ww . cournera-org/locture/nachine- learning-duke/cnnnath-model-isBMu.

[24.] Actization Functions in Neurd Networks. httpa://torardadatascionce con/activationfunctione-neural-notworke-1cbd9fgd91d6.

[25.] Conodutional Nend Netmorks in Python with Keras, ht tpe://ww-datacanp - con/conumity/ tutoriala/ convolutional-naural-networks-python.

[26.] Confusoun Matrix in Madine Lawning. ht tpa://nachinalaarningmastery . con/coafusionatrix-machine-learning/- Useful Pots to Diapnose your Neural Network. httpa :// towardudatarcience. com/usefulplotg-to-diagnoge-your-naural-notwark-521907fa2f45.

[27.] Bhandari, A., Koppen, J. & Agzarian, M (2020) Convolutional neural networks for brain tumour segmentation. Insights Imaging 11, 77. https://doi.org/10.1186/s13244-020-00869-4

[28.] Jin KH, McCann MT, Froustey E, Unser M (2017) Deep convolutional neural network for inverse problems in imaging. IEEE Trans Image Process 26: 4509–4522

[29.] Yamashita R, Nishio M, Do RKG, Togashi K (2018) Convolutional neural networks: an overview and application in radiology. Insights Imaging 9:611–629

[30.] Angulakshmi M, Lakshmi Priya GG (2017) Automated brain tumour segmentation techniques— a review. Int J Imaging Syst Technol 27:66–77

[31.] Paithane, P. M., & Kakarwal, D. (2022). Automatic Pancreas Segmentation using A Novel Modified Semantic Deep Learning Bottom-Up Approach. International Journal of Intelligent Systems and Applications in Engineering, 10(1), 98–104. https://doi.org/10.18201/ijisae.2022.272

[32.] Best B, Nguyen HS, Doan NB et al (2019) Causes of death in glioblastoma: insights from the SEER database. J Neurosurg Sci 63:121–126

[33.] Mikołajczyk A, Grochowski M (2018) Data augmentation for improving deep learning in image classification problem. 2018 International Interdisciplinary PhD Workshop (IIPhDW), pp 117-122

[34.] Chang K, Beers AL, Bai HX et al (2019) Automatic assessment of glioma burden: a deep learning algorithm for fully automated volumetric and bidimensional measurement. Neuro Oncol 21:1412–1422

[35.] Isensee F, Kickingereder P, Wick W, Bendszus M, Maier-Hein KH (2017) Brain tumor segmentation and radiomics survival prediction: contribution to the brats 2017 challenge. International MICCAI Brainlesion Workshop. Springer, pp 287-297

[36.] Perkuhn M, Stavrinou P, Thiele F et al (2018) Clinical evaluation of a multiparametric deep learning model for glioblastoma segmentation using heterogeneous magnetic resonance imaging data from clinical routine. Invest Radiol 53:647–654

[37.] Kumar, S., Gornale, S. S., Siddalingappa, R., & Mane, A. (2022). Gender Classification Based on Online Signature Features using Machine Learning Techniques. International Journal of Intelligent Systems and Applications in Engineering, 10(2), 260–268. Retrieved from https://ijisae.org/index.php/IJISAE/article/view/2020

[38.] Arunachalam M, Royappan Savarimuthu S (2017) An efficient and automatic glioblastoma brain tumor detection using shift-invariant shearlet transform and neural networks. Int J Imaging Syst Technol 27:216–226

[39.] Hasan SMK, Linte CA (2018) A modified U-Net convolutional network featuring a Nearest-neighbor Re-sampling-based Elastic-Transformation for brain tissue characterization and segmentation. Proc IEEE West N Y Image Signal Process Workshop 2018

[40.] Sundararajan R SS, Venkatesh S, Jeya Pandian M (2019) Convolutional neural network based medical image classifier. International Journal of Recent Technology and Engineering

[41.] Albadawy EA, Saha A, Mazurowski MA (2018) Deep learning for segmentation of brain tumors: impact of cross-institutional training and testing: Impact. Med Phys 45:1150–1158

[42.] Chang J, Zhang L, Gu N et al (2019) A mix-pooling CNN architecture with FCRF for brain tumor segmentation. J Visual Comm Image Represent 58: 316–322

[43.] Havaei M, Davy A, Warde-Farley D et al (2017) Brain tumor segmentation with deep neural networks. Med Image Anal 35:18 –31

[44.] Naceur MB, Saouli R, Akil M, Kachouri R (2018) Fully automatic brain tumor segmentation using end-to-end incremental deep neural networks in MRI images. Comput Methods Programs Biomed 166:39 –49

[45.] N. A. Libre. (2021). A Discussion Platform for Enhancing Students Interaction in the Online Education. Journal of Online Engineering Education, 12(2), 07–12. Retrieved from

_____

http://onlineengineeringeducation.com/index.php/joee/article/view/49

[46.] Sanghani P, Ang BT, King NKK, Ren H (2018) Overall survival prediction in glioblastoma multiforme patients from volumetric, shape and texture features using machine learning. Surg Oncol 27:709 –714

[47.] Lopez CJ, Nagornaya N, Parra NA et al (2017) Association of radiomics and metabolic tumor volumes in radiation treatment of glioblastoma multiforme. Int J Radiat Oncol Biol Phys 97:586 –595

[48.] Osman AFI (2019) A multi-parametric MRI-based radiomics signature and a practical ML model for stratifying glioblastoma patients based on survival toward precision oncology. Front Comput Neurosci 13:58.

[49.] Alaria, S. K. "A.. Raj, V. Sharma, and V. Kumar."Simulation and Analysis of Hand Gesture Recognition for Indian Sign Language Using CNN"." International Journal on Recent and Innovation Trends in Computing and Communication 10, no. 4 (2022): 10-14.

[50.] Dogiwal, Sanwta Ram, Y. S. Shishodia, Abhay Upadhyaya, Hanuman Ram, and Satish Kumar Alaria. "Image Preprocessing Methods in Image Recognition." International Journal of Computers and Distributed Systems 1, no. 3 (2012): 96-99.

[51.] Ashish Raj, Vijay Kumar, Satish Kumar Alaria, Vivek Sharma,. 2022. "Design Simulation and Assessment of Prediction of Mortality in Intensive Care Unit Using Intelligent Algorithms". Mathematical Statistician and Engineering Applications 71 (2):355-67. https://doi.org/10.17762/msea.v71i2.97

[52.] Deepali Koul, Satish Kumar Alaria. 2018. "A New Palm Print Recognition Approach by Using PCA &Amp; Gabor Filter". International Journal on Future Revolution in Computer Science &Amp; Communication Engineering 4 (4):38-45.

[53.] Rajput, B. S. ., Gangele, A. ., & Alaria, S. K. . (2022). Numerical Simulation and Assessment of Meta Heuristic Optimization Based Multi Objective Dynamic Job Shop Scheduling System. International Journal on Future Revolution in Computer Science &Amp; Communication Engineering, 8(3), 92–98.

[54.] Rajput, B. S. ., Gangele, A. ., Alaria, S. K. ., & Raj, A. . (2022). Design Simulation and Analysis of Deep Convolutional Neural Network Based Complex Image Classification System. International Journal on Future Revolution in Computer Science &Amp; Communication Engineering, 8(3), 86–91.